

# Surface Preparation of Silicon for Polymer Adsorption Studies

Peter Frantz and Steve Granick\*

Department of Materials Science and Engineering, University of Illinois,  
Urbana, Illinois 61801

Received September 25, 1991. In Final Form: January 15, 1992

The silicon surfaces that result from common preparation methods were evaluated on the basis of purity, reproducibility, and stability for use as a substrate in adsorption studies. Comparisons concerned (i) resulting adsorption-desorption kinetics of polystyrene adsorbed from cyclohexane solution near the  $\theta$  temperature, (ii) the surface interaction parameter ( $\chi_s$ ) inferred from displacement experiments, and (iii) the surface chemistry measured by surface analytical techniques. Subtle differences in surface chemistry induced large undesirable variations in dynamics. These differences showed up in the rates of (i) conformational equilibration and (ii) exchange between the adsorbed state and free solution, but not in the steady-state mass adsorbed onto an initially-bare silicon surface. Freshly etched surfaces were unstable over periods of hours. The most consistent results were obtained by exposing the silicon to oxygen plasma or ultraviolet radiation, such that formation of the homogeneous silicon oxide was favored.

## Introduction

Many recently developed techniques, designed to study the equilibrium properties of adsorbed macromolecules, have provided new stepping stones for our understanding of this complex phenomenon.<sup>1,2</sup> Yet, many more questions have been raised than satisfied. A point in understanding has been reached where one may no longer avoid questions about the kinetic and dynamic processes of adsorption.<sup>3</sup>

The bulk of experimental work has involved the physisorption of macromolecules from solution onto a solid substrate. Silicon and colloidal silica have been used in an immense number of adsorption studies owing to their well-characterized properties,<sup>4-6</sup> industrial relevance, affinity for molecular adsorption, and transparency in the infrared.

In our laboratory we have learned that the requirements to obtain reproducible dynamic data are much greater than to obtain this data regarding steady state. Subtle changes in the surface chemistry may strongly affect the rate of exchange, the rate of conformational equilibration, and possibly other kinetic quantities. To ensure the quantitative reproducibility of such measurements, a well-characterized and easily reproducible surface must be sought.

The obvious place to look for the proper method was in the literature of the semiconductor industry. In this vast and scattered literature,<sup>7</sup> one finds common ground only in the "RCA Standard Clean"<sup>8,9</sup> and its descendants, such as centrifugal spray cleaning<sup>10</sup> and so-called megasonic

cleaning.<sup>11</sup> Each researcher seems to have developed a unique method for his or her very specific purposes. These typically differ in the chemistry and temperature of the etchant solution, the time of exposure to this etchant, and the extent to which oxidation is allowed or encouraged. After the following brief recapitulation of the literature, our experiences using these methods to investigate the dynamics of polymer adsorption and displacement dynamics will be presented.

**Chemical Etching of Silicon.** Chemical etching methods are variations on the following framework. First, the surface is degreased to remove adsorbed hydrocarbons and other contaminants, leaving only the oxidized silicon (and, in some cases, adsorbed ions). Second, the remaining oxide is routinely removed by a brief bath in an etchant solution, usually hydrofluoric acid. From this step, physical and chemical heterogeneities may be expected to result, depending on the state of the oxide before etching and the choice of etchant solution. The common strategy to minimize such defects is to repeatedly grow and then strip the oxide layer, often using a variety of methods. The researcher wishing to study adsorption onto this surface must now promote the growth of siloxane or silanol groups.

A vast majority of chemical etchants are solutions of hydrofluoric acid.<sup>7-20</sup> The etched surface of Si(111) and Si(100) is ideally made up of silicon monohydride.<sup>12-14</sup> A 48% aqueous solution of hydrofluoric acid produces a surface with little long-range periodic order, as has been shown by atomic force microscopy (AFM),<sup>12</sup> Fourier transform infrared spectroscopy in attenuated total reflection (FTIR-ATR),<sup>13,14</sup> and electron energy loss spectroscopy (EELS).<sup>14</sup> Although this hydrogen-passivated

(1) Cohen-Stuart, M. A.; Cosgrove, T.; Vincent, B. *Adv. Colloid Interface Sci.* **1986**, *24*, 143.

(2) Kawaguchi, M. *Adv. Colloid Interface Sci.* **1990**, *32*, 1.

(3) Granick, S. In *Physics of Polymer Surfaces and Interfaces*; Sanchez, I., Ed.; Manning Publications: Greenwich, CT, in press.

(4) Cerofolini, G. F.; Meda, L. *Physical Chemistry of, in and on Silicon*; Springer-Verlag: New York, 1989.

(5) Iler, R. K. *The Chemistry of Silica*; John Wiley and Sons: New York, 1979.

(6) Hair, M. L. *Infrared Spectroscopy in Surface Chemistry*; Marcel Dekker, Inc.: New York, 1967.

(7) For reviews of semiconductor cleaning techniques, see: Kern, W.; Deckert, C. A. *Chemical Etching*. In *Thin Film Processes*; Vossen, J. C., Kern, W., Eds.; Academic Press: New York, 1978; Part v-1. Burkman, D. *Semicond. Int.* **1981**, *4*, 103.

(8) Kern, W.; Poutinen, D. A. *RCA Rev.* **1970**, *31*, 187.

(9) Kern, W. *RCA Engineer* **1983**, *28*, 99.

(10) Burkman, D. *Semicond. Int.* **1981**, *4*, 103.

(11) Mayer, A.; Swartzman, S. *J. Electron. Mater.* **1979**, *8*, 855.

(12) Kim, Y.; Liebler, C. M. *J. Am. Chem. Soc.* **1991**, *113*, 2333.

(13) Higashi, G. S.; Chabal, Y. J.; Trucks, G. W.; Raghavachari, K. *Appl. Phys. Lett.* **1990**, *57*, 1656.

(14) Burrows, V. A.; Chabal, Y. J.; Higashi, G. S.; Raghavachari, K.; Christman, S. B. *Appl. Phys. Lett.* **1988**, *53*, 998.

(15) Beckmann, K. H. *Surf. Sci.* **1966**, *5*, 187.

(16) Mende, G.; Finster, J.; Flamm, D.; Schulze, D. *Surf. Sci.* **1983**, *128*, 169.

(17) Massoud, H. Z.; Plummer, J. D.; Irene, E. A. *J. Electrochem. Soc.* **1985**, *132*, 2685.

(18) Abelson, J. Ph.D. Thesis, Stanford University, 1987.

(19) Tabe, M. *Appl. Phys. Lett.* **1984**, *45*, 1073.

(20) Ritter, J. C.; Robinson, M. N.; Faraday, B. J.; Hoover, J. I. *J. Phys. Chem. Solids* **1965**, *26*, 721.

surface is stable for several hours, the energetics for oxidation are slightly favorable. The rates of oxidation are increased at defect sites.<sup>4</sup> Common defects are dihydride, trihydride, and possibly some nonstoichiometric water.<sup>12-14</sup> Physical roughness has also been shown by metal oxide semiconductor (MOS) diode capacitance-voltage (*C-V*) and conductance-voltage (*G-V*) measurements.

To minimize these defects, one may lower the HF concentration or raise the pH. Chabal and co-workers<sup>13</sup> used FTIR-ATR to monitor the Si-H vibrations (2100  $\text{cm}^{-1}$ ) on a surface from which a thermally grown oxide had been stripped. The spectral peak was broad (30  $\text{cm}^{-1}$ ) when the surface was stripped by concentrated solution of HF in water (48%), but much sharper (10  $\text{cm}^{-1}$ ) when a 1-10% solution was used. The sharpening was attributed to a decreased density of dihydride and trihydride. Similar results were obtained by buffering the solution with  $\text{NH}_4$ . Lieber and co-workers<sup>12</sup> observed improvements in resolution of hexagonal symmetry, reproducibility, and stability, when HF solutions were buffered with  $\text{NH}_4$ .

**Oxidation of Etched Silicon.** A silicon hydride surface results from etching. It is necessary to replace this hydrogen surface layer with siloxane and/or silanol groups because the silicon hydride is chemically unstable and has low affinity for molecular adsorption. We recognize five categories of methods for promoting the growth of these functional groups. We suspect that more categories may exist.

A very common method employed by the semiconductor industry is thermal oxidation.<sup>17,20</sup> This requires temperatures in excess of 800 °C and was thus impractical for our purposes.

As mentioned above silicon hydride is prone to oxidize in air at room temperature.<sup>21</sup> The oxide thickness, *d*, grows according to the Elovich isotherm<sup>4,16</sup>

$$d = d_0 + r_0 t \ln(1 + t/\tau) \quad (1)$$

Here  $d_0$  is the initial thickness,  $\tau$  is a characteristic time, and  $r_0$  is the growth rate at  $t = 0$ . Although the estimated equilibrium oxide thickness is a healthy 1.4 nm, the long time constant and unavoidable possibilities for accompanying surface contamination make this method unattractive.

A recently developed oxidation technique is to expose the silicon to an ozone-rich environment.<sup>18,19</sup> The ozone may be generated electrochemically or by ultraviolet (UV) radiation from a low-pressure mercury lamp. The procedure of UV ozone cleaning will be described below. For a discussion of electrochemical ozone cleaning methods, the reader is referred to a paper by Baumgartner et al.<sup>22</sup> It should be remarked that the surface exposed to UV radiation has been claimed to suffer an order of magnitude more damage than with electrochemically generated ozone,<sup>22</sup> as no sputtering of the surface may occur; other researchers have not seen evidence of induced roughness, however.<sup>23</sup> We chose not to use the electrochemical method because experience has shown that chemical baths encourage contamination.

The reaction pathway for the cleaning of contaminants by UV ozone has not been established. Indeed, it is not yet known whether the UV radiation or the ozone is responsible. In a comprehensive discussion by Abelson,<sup>18</sup>

it is explained that the 254-nm line of mercury may itself effectively dissociate typical hydrocarbons. The 185-nm mercury line generates ozone through  $\text{O}_2 + h\nu(185\text{nm}) \rightarrow \text{O}(^3\text{P}) + \text{O}(^3\text{P})$  followed by  $\text{O}(^3\text{P}) + \text{O}_2 \rightarrow \text{O}_3$ , but the 254-nm line decays it via  $\text{O}_3 + h\nu(254\text{nm}) \rightarrow \text{O}_2 + \text{O}(^1\text{D})$ . On the other hand, it is certain that ozone oxidizes hydrocarbons to form CO and that surface oxidation is enhanced by active oxygen species  $\text{O}_3$  and  $\text{O}^{\cdot}$ .<sup>19</sup> Regardless of the process, experiments described in ref 18 showed that an exposure time of 5-30 min produces a surface that, characterized by Auger spectroscopy, is found to carry an oxide layer 1.5 nm thick and no carbon contamination. Table<sup>19</sup> showed that there is no further oxidation after the UV ozone treatment and that adsorption of carbon contaminants proceeds slowly, although no explanation for this stability was offered.

Another useful technique is bombardment of the silicon surface with oxygen ions. It was shown by Jorgensen<sup>24</sup> that some species of negative oxygen ion is the principal diffusing particle responsible for oxidation. The concentration of these ions is greatly increased in an oxygen plasma. An early investigation of this approach was performed by Ligenza.<sup>25</sup> In this study oxygen plasma, excited by a 300-W microwave discharge, displayed the spectral lines of atomic oxygen and  $\text{O}_2^+$ , but it was not possible to detect  $\text{O}^-$ . The surface of a dc silicon anode, acting as a Langmuir probe, developed an oxide layer of 600 nm in only 1 h at moderate temperatures. Without the application of an external voltage, oxidation occurred at a lower rate and reached a plateau of 450 nm. Auger spectra indicated no carbon on the surface, and it was subsequently shown that the substantial radiation damage may be minimized by maintaining the plasma at room temperature.<sup>26</sup>

The strong influence of surface hydroxyl groups on adsorption is well documented.<sup>6,27-29</sup> It is worthwhile to note that there are likely to be several types of hydroxyl groups on the surface. The most common are<sup>5</sup> isolated, freely vibrating SiOH groups (free hydroxyl groups), isolated pairs of SiOH groups bonded to each other (vicinal), and adjacent pairs of SiOH groups with hydrogens bonded to each other. It has been shown<sup>30</sup> that small molecules adsorb preferentially to the free hydroxyl groups. Due to the physical roughness of our surface, we must expect a distribution of all three types. The free hydroxyl groups must predominate at the peaks of the topography, while the isolated pairs must predominate in the valleys.<sup>5</sup>

Many methods are available to the researcher who wishes to enhance the growth of silanol groups on a silicon surface. We have chosen a few which will be described below. It is worth noting that many studies that employ silica<sup>31</sup> as a substrate are performed on fully hydroxylated surfaces.

## Experimental Section

The FTIR spectra were collected using a Nicolet IR/30 spectrometer in the mode of attenuated total reflection. The methods and calibrations are described elsewhere.<sup>32-34</sup>

(24) Jorgensen, P. J. *J. Chem. Phys.* 1962, 37, 874.

(25) Ligenza, J. R. *J. Appl. Phys.* 1965, 36, 2703.

(26) Bean, J. C.; Becker, G. E.; Petroff, P. M.; Seidel, T. E. *J. Appl. Phys.* 1977, 48, 1977.

(27) Kiselev, A. V. *Discuss. Faraday Soc.* 1971, 52, 14.

(28) Cusumano, J. A.; Low, J. D. *J. Phys. Chem.* 1970, 74, 1950.

(29) Griot, O.; Kitchener, J. A. *Trans. Faraday Soc.* 1965, 61, 1026.

(30) Davydov, V. Ya.; Kiselev, A. V.; Lygin, V. I. *Russ. J. Phys. Chem.* 1963, 37, 243.

(31) Huguenard, C.; Varoqui, R.; Pefferkorn, E. *Macromolecules* 1991, 24, 2226.

(32) Kuzmenka, D. J.; Granick, S. *Colloids Surf.* 1988, 31, 105.

(33) Johnson, H. E.; Granick, S. *Macromolecules* 1990, 23, 3367.

(34) Frantz, P.; Granick, S. *Phys. Rev. Lett.* 1991, 66, 899.

(21) Deal, B.; Grove, A. *J. Appl. Phys.* 1965, 36, 3770.

(22) Baumgartner, H.; Fuenzalida, V.; Eisele, I. *J. Appl. Phys.* 1987, 43, 223.

(23) Silberzan, P.; Leger, L.; Ausserre, D.; Benattar, J. J. *Langmuir* 1991, 7, 1647.

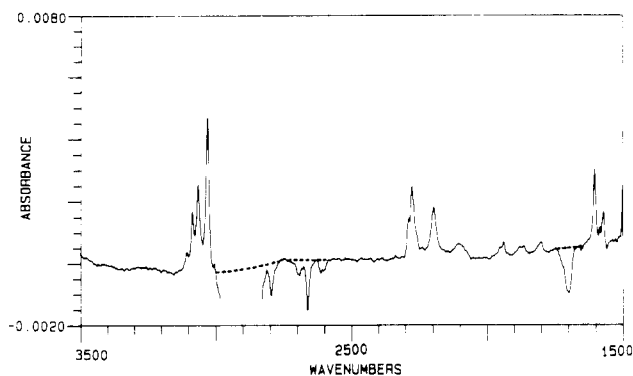


**Figure 1.** Infrared spectrum of PS-*h* and PS-*d* adsorbed jointly onto silicon from a cyclohexane solution of 0.1 mg/mL. Absorbance is plotted against wavenumbers. From the integrated intensities of the polystyrene C-H ring vibrations (3000–3150  $\text{cm}^{-1}$ ) and of the C-D vibrations (2000–2300  $\text{cm}^{-1}$ ), the surface excess plotted in succeeding figures is calculated. UV ozone cleaning was used to prepare the silicon substrate in this experiment.

**Table I. Characterization of the Polystyrenes (Suppliers' Data)**

sample	$M_w$	$M_w/M_n$	source
PS- <i>h</i>	575 000	1.06	Pressure Chemical
PS- <i>d</i>	550 000	1.05	Polymer Laboratories

The cylindrical internal reflection element was a single crystal silicon rod that had been polished with  $1/4\text{-}\mu\text{m}$  diamond paste.

Anionically polymerized atactic polystyrene (PS), protio (PS-*h*) and deuterio (PS-*d*) standards of similar degree of polymerization, were purchased and used as received. Their characteristics are listed in Table I. Polymer samples were dissolved in freshly distilled cyclohexane (Baker) at a concentration of 1.0 mg/mL. The experiments were thermostated at 30.0  $^{\circ}\text{C}$ , which is the  $\theta$  temperature ( $T_{\theta}$ ) for PS-*d* in cyclohexane. The PS-*h*,  $T_{\theta} = 34.5\text{ }^{\circ}\text{C}$ ,<sup>33</sup> therefore found itself in a slightly poorer solvent than did PS-*d*, as we have discussed previously.<sup>34</sup>

Figure 1 shows a representative spectrum of PS-*h* and PS-*d* adsorbed jointly. Absorbance is plotted against wavenumbers. Protio PS-*h* shows a series of carbon-hydrogen vibrations in the region 3000–3150  $\text{cm}^{-1}$ , and PS-*d* shows a series of carbon-deuteron vibrations in the region 2000–2300  $\text{cm}^{-1}$ . The negative peaks indicate the depletion of cyclohexane from the surface. The peaks in the region 1800–2000  $\text{cm}^{-1}$  are the carbon-carbon peaks common to both species.

In the displacement experiments, the displacer solvent was methylene chloride (Fisher Chemical).

## Results

**Surface Preparations.** The four different surface preparations presented below fall into the categories of wet chemistry, oxygen plasma treatment, and exposure to ozone generated by UV radiation. In addition, control experiments were performed on a surface that had only been etched by hydrofluoric acid immediately before use.

Because the surface chemistry is most affected by the final stages of the preparations, the initial steps, degreasing and stripping, were held constant. To remove organic contaminants, the silicon was first subjected to ultrasonic agitation in a bath of ethyl acetate. The oxide was then stripped by a dip, for 15 s, in a 5% aqueous solution of hydrofluoric acid. It was then thoroughly flushed with deionized water. No attempt to minimize the surface physical roughness was made.

The surface preparations methods are as follows.

**1. Chemical Etch Only.** This produced an oxide-deficient surface. Immediately after treatment with the HF solution, the substrate was dried in a jet of dry nitrogen

gas and quickly placed in a stainless steel cell. The time of exposure to the ambient laboratory atmosphere was less than 5 min. Similar results were obtained when the prism was dried in a vacuum oven instead.

**2. Acid Bath.** To promote the growth of surface silanol groups, two different chemical baths were concocted. The first, commonly known as a "piranha solution", is composed of 7:3  $\text{H}_2\text{SO}_4/30\%$   $\text{H}_2\text{O}_2$ . Please see ref 35 for precautions for handling this hazardous material. After 5 min in this solution, bubbles began to form on the surface of the prism. Experience showed that this indicated pitting of the silicon surface. The prism was quickly flushed with deionized water and dried in a jet of dry oxygen. The second method consisted of a 5-min dip in a saturated solution of KOH and 2-propanol. Rapid pitting of the surface was also observed in this bath, resulting in reduced infrared reflectance.

**3. UV Ozone Treatment.** A simple ozone chamber was constructed. A low-pressure mercury lamp, made with fused silica to transmit the 185-nm line, was purchased from BHK (Pomona, CA). Its nominal radiant flux at 254 nm is 12–15  $\text{mW}/\text{cm}^2$  at a distance of 1 in. The cylinder of silicon is held by its ends at a distance of 5 mm from the serpentine mercury vapor tube. The prism is slowly (0.2 rpm) rotated about its central axis to ensure even exposure to UV radiation. Oxygen is bled into the back of the aluminum chamber and is allowed to seep out through the front panel. Before use, the system is run for 30 min to clean itself. The prism is then quickly inserted and exposed to the UV ozone for 15 min. A separate investigation of contact angles of water on the treated surface of silicon wafers indicated, in agreement with ref 19, that this is the optimal exposure time. The contact angle of water on the (111) face was minimized by limiting the exposure to a similar amount of time.

**4. Oxygen Plasma.** A plasma chamber (PDC-32G) was purchased from Harrick (Ossining, NY) and run with a reduced pressure ( $1/10$  Torr) oxygen atmosphere. The plasma, maintained by a 100-W radio frequency discharge, is contained in a cylindrical quartz chamber. Immediately after etching, the silicon was sealed in the chamber and exposed to the plasma for 5 min. It was allowed 10 min to cool and equilibrate in the reduced pressure oxygen before installation in the stainless steel ATR cell.

**Exchange and Displacement Experiments.** Two types of FTIR experiments were performed with each category of surface preparation. These will be called the exchange experiment and the displacement experiment.

Figure 2 illustrates the sequence of the exchange experiment. Initially (time  $t = 0$ ), a solution containing PS-*h* was admitted into the ATR cell. Although it quickly reached steady state in total mass adsorbed, we allowed 6 h for (slow) conformational equilibration, for reasons discussed elsewhere.<sup>34</sup> This solution was then replaced by the isotopically labeled PS-*d* solution. The desorption of PS-*h*, and concomitant adsorption of PS-*d*, was followed. The differential sticking energy, favoring adsorption of PS-*d*, was previously characterized as small ( $\sim 0.03$  kT) per repeat unit,<sup>36</sup> but large per chain molecule. In addition to this energetic drive toward exchange, exchange was also driven entropically because concentration of the adsorbate in the bulk solution is essentially zero. It is possible to make precise measurements of the rates of exchange and the surface excess of both species before and after

(35) Bain, C. D.; Evall, J.; Whitesides, G. J. *Am. Chem. Soc.* **1989**, *111*, 7155.

(36) Frantz, P.; Leonhardt, D. C.; Granick, S. *Macromolecules* **1991**, *24*, 1868.

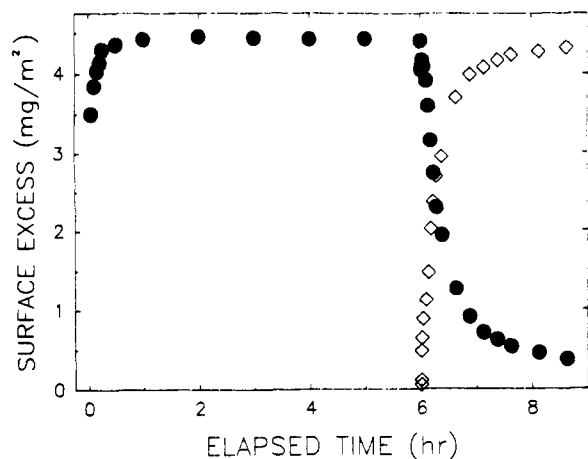


**Figure 2.** An illustration of the sequence of each exchange experiment. UV ozone cleaning was used to prepare the silicon substrate in this experiment. Surface excess ( $\text{mg}/\text{m}^2$ ) is plotted versus time. First PS-*h* solution ( $1 \text{ mg mL}^{-1}$ ,  $M_w = 575\,000$ ) was exposed to the silicon surface. After a waiting time, commonly 6 h, this solution was replaced by PS-*d* solution ( $1 \text{ mg mL}^{-1}$ ,  $M_w = 550\,000$ ) and the ensuing adsorption-desorption kinetics were monitored.

exchange, and the shape of the desorption curve gives information about the distribution of chain conformations at the surface.

**Adsorption Isotope Effect.** Our earlier determination of the adsorption isotope effect, which favors adsorption of deuterio PS,<sup>36</sup> concerned adsorption onto oxidized silicon. Control experiments, involving adsorption onto silicon that had undergone an HF etch only, confirmed the generality of the earlier results regardless of the surface preparation.

**Evaluation of the  $\chi_s$  Parameter.** The displacement experiment allows one to estimate segmental adsorption energies, characterized by a  $\chi_s$  parameter. This parameter, introduced by Silberberg,<sup>37</sup> is defined as the difference in dimensionless adsorption energy (kT) between a polymer segment and a solvent molecule. The segmental adsorption energy may be decreased by adding a monomeric displacer to the polymer-solvent solution,<sup>38</sup> to give a displacer volume fraction  $\phi_d$ . At a certain displacer volume fraction, termed the critical volume fraction  $\phi_c$ , the polymer is completely displaced. An elegant technique, developed by Cohen-Stuart et al.,<sup>38</sup> provides a relationship between this point and the segmental adsorption energy. The interested reader is referred to a paper by van der Beek et al.<sup>39</sup> for a practical description and application of this theory.

Estimates of the  $\chi_s$  parameter were made to compare the effects of the different methods of surface preparation. As in the original theory, athermal conditions were assumed for computational simplicity and to minimize parameters. Errors incurred by this approximation were calculated in ref 40 to be commonly less than 5% of the  $\chi_s$  value. In any event, the errors incurred by ignoring all permutations of interactions between polymer, solvent, and displacer may be expected to be the same regardless of surface preparation method, and so this approximation is particularly justified insofar as one is interested primarily in the differences (not the absolute value) of the segmental

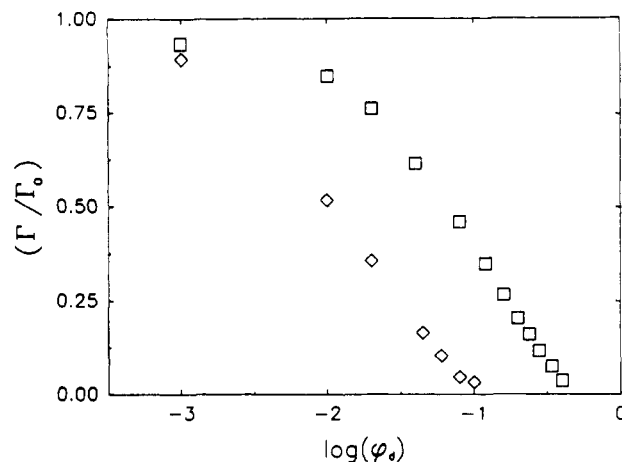


**Figure 3.** Displacement experiments performed on the etched silicon surfaces (surface preparation method 1). Surface excess of PS-*h*, normalized by the surface excess prior to addition of  $\text{CH}_2\text{Cl}_2$ , is plotted against logarithmic volume fraction  $\text{CH}_2\text{Cl}_2$ : diamonds, 30-min aging time; squares, 12-h aging time. The increase of the critical displacer volume fraction ( $\phi_{cr}$ ) with increasing aging time corresponds, by eq 2, to segmental adsorption energies of 1.7 and 2.2 kT, respectively (see text).

adsorption energy. Under athermal conditions, the segmental adsorption energy may be expressed as<sup>39</sup>

$$\chi_s = \ln \{ \phi_{cr} \exp[\alpha' A(\epsilon_d - \epsilon_o)] + 1 - \phi_{cr} \} + \chi_{sc} \quad (2)$$

Here, as described in ref 41,  $\chi_{sc}$  is the critical adsorption energy: the minimum value of  $\chi_s$  for which long chains adsorb from the solvent. For a hexagonal lattice,  $\chi_{sc} = 0.288$ . The parameter  $\alpha'$  is the activity of the substrate and is roughly  $18 \text{ nm}^{-2}$  for silica. (Note, however, that strictly speaking this quantity may not remain constant throughout changes in the surface preparation.) The parameters  $\epsilon_o$  and  $\epsilon_d$  are the solvent strengths of the pure solvent and the pure displacer, respectively. They are given as  $\epsilon_o = 0.04$  and  $\epsilon_d = 0.30$ . The mean molecular area ( $A$ ) is  $0.48 \text{ nm}^2$ .

In the spirit of conservation of material, no polymer was dissolved in our solvent/displacer solutions. In view of the long equilibration time for the entropically driven desorption of polymer into the pure solution,<sup>1</sup> and the restriction of our interest to the critical point  $\phi_c$ , this will introduce no complications.

Figure 3 shows typical displacer experiments. Details of the two experiments presented are described later. The polymer solution is admitted into the ATR cell, and ample time is allowed for equilibration. To obtain a value of the surface excess at infinite dilution, the polymer solution is replaced by pure solvent. This data point is treated as displacer volume fraction  $\phi_d = 1 \times 10^{-3}$  for purposes of logarithmic plots, since control experiments using that volume fraction showed findings indistinguishable from  $\phi_d = 0$ . The displacer volume fraction was then incremented until the C-H peaks were no longer visible. The volume fraction at which these points extrapolate to the  $\phi$  axis is then  $\phi_{cr}$ . It appears, in Figure 3, that the data points of the highest volume fractions (lowest surface excess) fall to the right of the line extrapolated from the points of lower volume fraction. As is explained in ref 41, this is to be expected, and the appropriate  $\phi_c$  is to be taken as the intersection of the extrapolated line and the  $\phi$  axis.

**Results of Preparation 1.** Figure 4 shows results of three exchange experiments performed on the etched

(37) Silberberg, A. *J. Chem. Phys.* 1968, 48, 2836.

(38) Cohen Stuart, M. A.; Fler, G. J.; Scheutjens, J. M. H. M. *J. Colloid Interface Sci.* 1984, 97, 515.

(39) van der Beek, G. P. *Macromolecules* 1991, 24, 6600.

(40) van der Beek, G. P.; Cohen Stuart, M. A.; Fler, G. J.; Hofman, J. E. *Langmuir* 1989, 5, 1180.

(41) van der Beek, G. P.; Cohen Stuart, M. A.; Fler, G. J. *Macromolecules* 1991, 24, 3553.

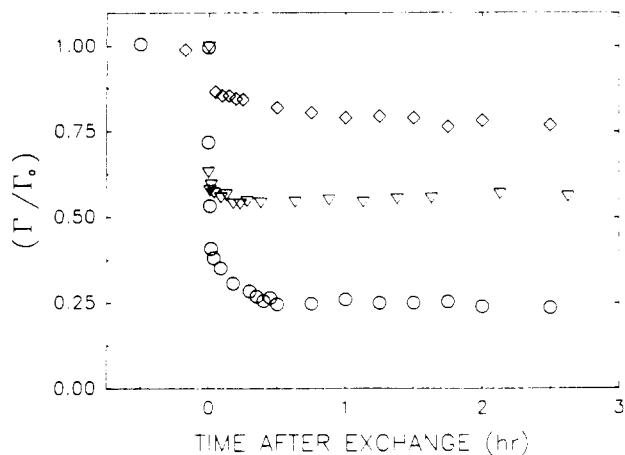


**Figure 4.** Exchange experiments performed using a silicon surface that had been etched only (surface preparation method 1). Time-dependent surface excess, normalized by the surface excess of PS-*h* prior to exchange, is plotted against elapsed time after exchange of solutions. The surface was allowed different aging times before the exchange: diamonds, 12 h; triangles, 6; circles, 30 min.

surface prepared by the first method described above. The values of surface excess, for each experiment, were within 10% of each other. Surface excess of PS-*h*, normalized by the surface excess before exchange, is plotted against time after exchange of PS-*h* for PS-*d* solution.

The experiments in Figure 4 differ in the amount of time that the initial layer (PS-*h*) was allowed to reside on the surface before being challenged by PS-*d*. Consider the set of data for which the PS-*h* residence time before exchange was 30 min. The exchange proceeded very quickly; more than 80% of the PS-*h* was evacuated within 30 min, leaving only a small residual trapped fraction. The rapid time constant and the large degree of exchange indicate a relatively homogeneous distribution of loosely adsorbed PS-*h*.

Other experiments in Figure 4 represent PS-*h* residence times of 6 and 12 h, respectively. The desorption data again split into a period of rapid desorption, followed by minimal further desorption. Any changes that may have occurred in the initial rate of desorption were too small to be resolved. However, a significant reduction in the total amount of PS-*h* desorbed, and of PS-*d* adsorbed, is obvious with increasing residence time. As the system aged, larger fractions of the adsorbed layer became tightly bound. It appears that the increase of the tightly bound, or kinetically blocked, fraction may saturate to a level around 0.75.

This is supported by the displacement experiments shown in Figure 3. The two experiments displayed represent aging times of 30 min and 12 h. The increase of the critical displacer volume fraction ( $\phi_{cr}$ ), with increasing aging time, correspond, by eq 1, to  $\chi_{sc}$  approximately 1.7 and 2.2 kT for the 30-min and 12-h systems, respectively.

The likely explanation for these findings is that at the beginning of each experiment the freshly stripped surface contained little oxide, hence few potential adsorbing sites. As the surface was allowed to age in the solution, trace amounts of water may have slowly hydrated the silicon hydride surface. As this proceeded, polymers would adsorb to the resulting surface silanols. In the discussion below, this scenario will be developed further by including information from the next surface preparation.

We stress that this aging is not a result of slow conformational equilibration of the adsorbed layer. Such

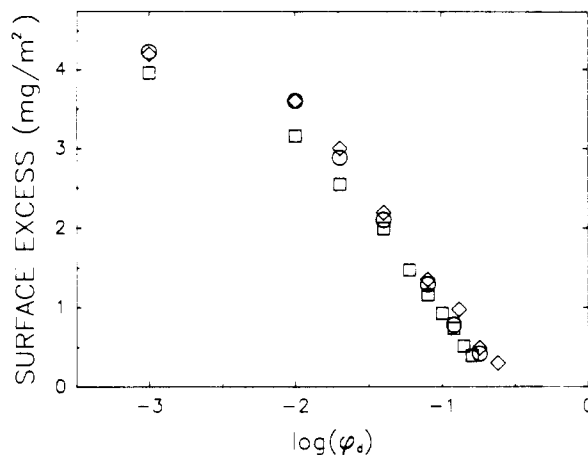


**Figure 5.** Displacement experiments performed using oxidized silicon surfaces (surface preparation methods 3 and 4). Surface excess of PS-*h*, normalized by the surface excess prior to addition of  $\text{CH}_2\text{Cl}_2$ , is plotted against logarithmic volume fractions  $\text{CH}_2\text{Cl}_2$ : circles, oxygen plasma preparation, 6 h; diamonds, UV ozone preparation, 6 h. The critical displacer volume fraction ( $\phi_{cr}$ ) is close to that observed using surface preparation method 1 and 30-min aging (squares), indicating a similar segmental adsorption energy on the order of 2.1 kT.

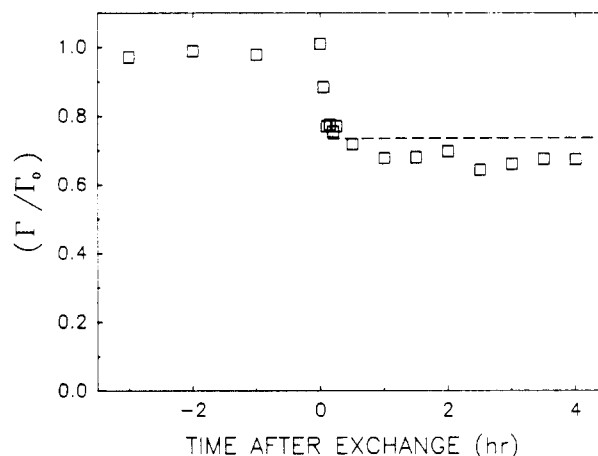


**Figure 6.** An exchange experiment performed on a silicon surface treated with piranha solution (surface preparation method 2). Time-dependent surface excess, normalized by the surface excess of PS-*h* prior to exchange, is plotted against elapsed time after exchange of solutions. The dashed line represents the approximate level of trapped surface excess at 12 h from Figure 4.

rearrangements, described elsewhere,<sup>34</sup> may also be expected to affect the rates of exchange.<sup>34</sup>

In support of this, we observed no changes, with aging, of the  $\chi_{sc}$  of the oxidized surfaces (preparations 3 and 4). The data are presented in Figure 5, which compares aging times of 30 min and 6 h. Figure 5 is discussed further below.

**Results of Preparation 2.** The second preparation recipe was intended to produce a densely hydrated surface. A typical exchange experiment performed on this substrate is shown in Figure 6. Surface excess of PS-*h*, normalized by the surface excess before exchange, is plotted against time after exchange of PS-*h* for PS-*d* solution. Again there are loosely and tightly bound fractions, with a trapped fraction (0.68) similar to the "etched only" surface at long aging time (Figure 4). It has been shown that the surface concentration of silanol groups, the silanol number ( $\alpha_{OH}$ ), is a physicochemical constant for a fully hydroxylated surface.<sup>42</sup> Comparison with the data of Figure 4 at long aging times, where a hydrated surface was presumed to

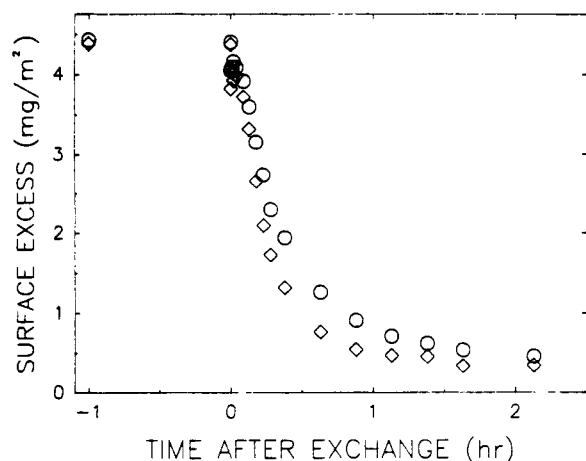


**Figure 7.** Exchange experiments performed using oxidized silicon surfaces (surface preparation methods 3 and 4). Time-dependent surface excess, normalized by the surface excess of PS-*h* prior to exchange, is plotted against elapsed time after exchange of solutions: circles, oxygen plasma preparation; diamonds, UV ozone preparation.

have developed, supports the view that the surface had been largely hydrated.

An exchange experiment after a 5-min dip in KOH/2-propanol produced unusually noisy and spurious data. A second attempt at this approach (1-h dip) only served to badly damage the surface. It was necessary to repolish the prism, and this method was aborted.

**Results of Preparations 3 and 4.** Results using preparations 3 and 4 are compared in Figure 7. The surface excess of PS-*h*, normalized by the surface excess before exchange, is plotted against time after exchange of PS-*h* for PS-*d* solution. The data represented by diamonds refer to an exchange experiment performed using a surface prepared using UV ozone exposure; the circles refer to plasma treatment. The exchange kinetics are remarkably similar in both cases. In addition, displacement experiments were performed on these surfaces, as shown in Figure 5, and virtually identical results were obtained. Due to the apparent similarities in both kinetics and steady-state levels of surface excess, these two preparation methods will be treated concurrently in this discussion.

The exchange kinetics are significantly different from those obtained using the hydrated oxide surface. Particularly noteworthy is that desorption continued until nearly all of the initial species (PS-*h*) had been removed. The entire range of the IR spectrum was clean and stable throughout the 14-h experiment, unlike our experience using surface preparation methods 1 and 2. In addition, we found excellent reproducibility between independent experiments, both in the total levels adsorbed and in the rates of exchange.

The segmental adsorption energy of PS-*h* on this surface was inferred to be approximately 2.1 kT. This is only 0.1 kT less than that of the fully hydrated surface. Therefore, it is apparent that although the segmental adsorption energy of two surfaces may be quite similar, kinetic processes (i.e., compare Figures 2, 4, and 6) may be very different.

In Table III,  $\chi_{sc}$  values for each of the surface preparations mentioned above are collected.

**Surface Analysis.** Preparations 1 and 3 were compared by Auger, XPS, and LEED analysis of the (111) face of a silicon wafer using the facilities of the Center for Microanalysis at the Materials Research Laboratory of

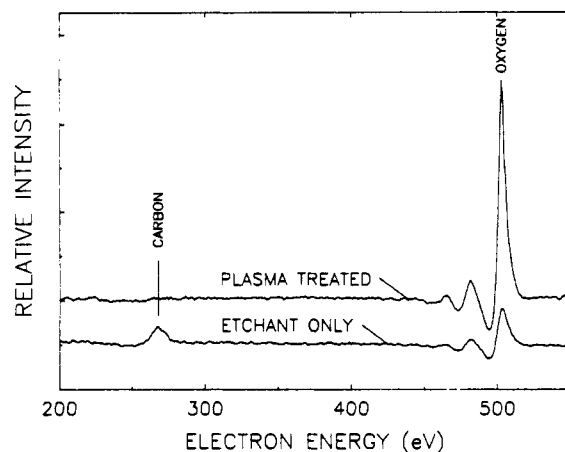


**Figure 8.** Auger spectra of the (111) face of a silicon wafer. One of these had been treated with oxygen plasma (surface preparation method 3); the other had been etched only (surface preparation method 1).

**Table II.**  $\chi_{sc}$  Values for Different Surface Preparations<sup>a</sup>

surface treatment	$\chi_{sc}$	surface treatment	$\chi_{sc}$
HF etch only (30 min)	1.7	oxygen plasma	2.1
HF etch only (12 h)	2.2	UV ozone	2.1
KOH (base bath)	2.2		

<sup>a</sup> Evaluated from displacement experiments using eq 2.

**Table III.** Relative Compositions by XPS<sup>a</sup>

surface treatment	C(1s)	O(1s)	Si(2p)	[O]/[SiO]
HF etch only	26.8	8.45	64.74	very large
oxygen plasma	7.6	46.69	45.69	5.3
KOH (base bath)	15.2	37.81	46.99	6.9
UV ozone	15.4	42.96	41.61	3.2

<sup>a</sup> Note: incidence angle was 45°.

the University of Illinois. We are indebted to John Peanasky and to Professor A. J. Gellman for assistance with these measurements.

The Auger spectra of an oxygen-plasma-treated silicon wafer is compared to that of an HF etched wafer in Figure 8. Auger measurements were performed on a Perkin-Elmer 15-120 Auger spectrometer with LEED optics, in the laboratory of Prof. A. J. Gellman. The relative intensity of Auger peaks is plotted against electron energy. The spectra clearly show the depletion of carbon contaminants and the acquisition of an oxide layer after plasma treatment. After plasma treatment, no diffraction pattern could be obtained using LEED, indicating that the oxide was aperiodic.

Table II shows results of XPS measurements of surfaces prepared in four different ways. The samples were introduced into a PHI 5400 X-ray photospectrometer immediately after cleaning, and analyzed with a Mg unmonochromatized X-ray source. Relative composition of C (1s peak), O (1s peak), and Si (2p peak) are listed, together with the ratio [O]/[SiO]. The angle of incidence was 45°. The results support the picture of little carbon organic contamination and that a robust oxide resulted from preparations 3 and 4.

In view of the literature reviewed in the Introduction, especially refs 18, 24, and 25, we are confident that the oxide developed by preparations 3 and 4 is composed primarily of SiO<sub>2</sub>. Some SiOH may have also become incorporated in the course of the plasma treatment due to sputtered water that had been adsorbed on the inner walls of the plasma chamber.<sup>43</sup> In the data shown in Table

II, the slightly higher ratio of [O] to [SiO] for preparation 4 than for preparation 3 may be an indication of this effect.

### Discussion of Kinetic Differences

There are striking qualitative differences in exchange kinetics between the pure oxide surfaces (preparations 3 and 4) and the hydrated oxide surfaces (presumed to result from preparations 1 and 2). Due to the initial conditions of the PS-*h* layer on the hydrated surface, we observed two distinct populations of desorbing polymer: one with an immeasurably brief desorption time constant and one which seemed to be interminably attached. The polymer that desorbs from a surface that is blanketed by a pure oxide layer acts as a single population of slowly desorbing chains.

On a cautionary note, it is crucial to realize that these differences are not due merely to a different intensity of interaction with the surface. They must also be dramatically affected by the spectrum of chain conformations, by the specificity of the interactions, and by the homogeneity of the substrate, all of which also depend on the surface preparation. Kinetics are also influenced by the nature of the invading species, which was held constant in this study.

We note, moreover, that steric impedence, both by neighboring chains and by the incoming traffic during exchange, may also serve as a hindrance to the desorption process.<sup>46</sup> The number and effectiveness of steric obstructions—a sort of entanglement—should depend on the surface preparation as mentioned above.

It was remarked earlier that the shape of the desorption curve may contain information about the distribution of chain conformations. At the same time, the shape of the displacement curves may contain information about the heterogeneities of the surface. We suspect that the leveling off of the displacement curve—concavity in the slope during the final stages of the experiment—may be caused by a population of chains that are attached to tightly binding surface heterogeneities. This effect, which is more pronounced in some studies<sup>44</sup> than in others,<sup>41</sup> is also vaguely apparent in the curves of Figure 5.

Ideally, in order to obtain a more thorough character-

(43) Nuzzo, R. Private communication.

ization of the surfaces described in this study, one would also monitor the spectroscopic bands corresponding to the relevant surface species such as SiOH, SiO<sub>2</sub>, and SiH, as described in the Introduction. This would require greater sensitivity than is allowed by the optics employed in this study. We have, however, achieved our goal of producing a stable and reproducible surface.

### Conclusion

We offer this study as a cautionary note to those who would use silicon, or a related substrate such as silica,<sup>5</sup> to investigate the time dependence of polymer adsorption. While there are no finer candidates for a common model surface for such studies, it is clear that the few nanometers of surface chemistry are far more important than the monolithic body of silicon that supports it. The present study has employed polycrystalline substrates. Though these might be expected to be rough, hydrofluoric acid etches defects preferentially to the Si(111) face, effectively exposing and smoothing this plane.<sup>45</sup> The delicate sensitivity that is required for measurements of dynamic phenomena has brought us into a regime where one may be inadvertently observing subtle heterogeneities in the chemistry of the surface. With such sensitivity and abundance of surface treatments, comparison with nominally similar studies in the literature may be questionable.

We found that common surface hydration methods (e.g., acid bath) are prone to cause contamination and, especially, damage of the substrate.

In the work reported here, the most successful strategy to minimize surface heterogeneities was to blanket them with a homogeneous layer of oxide.

**Acknowledgment.** We are indebted to J. Peanasky, A. J. Gellmann, and R. Nuzzo for collaborations and discussions regarding the work cited here. Support was provided through the National Science Foundation (Polymers Program), Grant NSF-DMR-91-01509.

**Registry No.** PS, 9003-53-6; Si, 7440-21-3; HF, 7664-39-3; KOH, 1310-58-3; *i*-PrOH, 67-63-0.

(44) Kawaguchi, M.; Chikazawa, M.; Takahashi, A. *Macromolecules* 1989, 22, 2195.

(45) Jakob, P.; Chabal, Y. J. *J. Chem. Phys.* 1991, 95, 2897.

(46) Johnson, H. E.; Granick, S. *Science* 1992, 255, 966.